

Electric Field Effects on Graphene Materials

Elton J. G. Santos

Abstract Understanding the effect of electric fields on the physical and chemical properties of two-dimensional (2D) nanostructures is instrumental in the design of novel electronic and optoelectronic devices. Several of those properties are characterized in terms of the dielectric constant which play an important role on capacitance, conductivity, screening, dielectric losses and refractive index. Here we review our recent theoretical studies using density functional calculations including van der Waals interactions on two types of layered materials of similar two-dimensional molecular geometry but remarkably different electronic structures, that is, graphene and molybdenum disulphide (MoS_2). We focus on such two-dimensional crystals because of their complementary physical and chemical properties, and the appealing interest to incorporate them in the next generation of electronic and optoelectronic devices. We predict that the effective dielectric constant (ϵ) of few-layer graphene and MoS_2 is tunable by external electric fields (E_{ext}). We show that at low fields ($E_{\text{ext}} < 0.01 \text{ V/\AA}$) ϵ assumes a nearly constant value ~ 4 for both materials, but increases at higher fields to values that depend on the layer thickness. The thicker the structure the stronger is the modulation of ϵ with the electric field. Increasing of the external field perpendicular to the layer surface above a critical value can drive the systems to an unstable state where the layers are weakly coupled and can be easily separated. The observed dependence of ϵ on the external field is due to charge polarization driven by the bias, which show several similar characteristics despite of the layer considered. All these results provide key information about control and

Elton J. G. Santos^{†,*}

School of Engineering and Applied Sciences, Harvard University, Cambridge, Massachusetts 02138, USA.

[†]Present address: Department of Chemical Engineering, Stanford University, Stanford, California 94305, USA.

*e-mail: eltonjos@stanford.edu

understanding of the screening properties in two-dimensional crystals beyond graphene and MoS₂.

1 Introduction

Electron-electron interactions play a central role on a wide range of electronic phenomena in two-dimensional (2D) materials. One of the main ingredients that determines the Coulomb interaction strength in those systems is screening, which can be characterized by dielectric constant, ε . Indeed, screening effects based on ε play a fundamental role in determining the electron dynamics, the optical exciton binding energy, the electron and hole mobilities as well as charge storage features. In this context the Coulomb interactions are confined in a two-dimensional geometry which can give place to a new set of dielectric properties depending on the electronic nature of the 2D crystal.

Graphene, a semimetal with zero bandgap, and MoS₂, a low-dimension direct band gap semiconductor, are two representative members of the 2D family that have been receiving much attention in many fields due to their remarkable chemical and physical properties (Castro Neto et al. 2009, Wang et al. 2012). One of the main features that influences all these properties is the layer thickness, which determines the charge distribution in the device as well as the electronic structure through the band gap. In particular, graphene can become a semiconductor with a band gap of several tenths of meV's at a bilayer structure subjected to high electric gate bias (Castro et al. 2007). MoS₂, in its turn, has a sizable band gap that varies as a function of the number of layers which reaches values of about 1.8 eV at the monolayer limit (Mak et al. 2010). In both situations the electric-field screening is observed to change as the dielectric response depends on the intrinsic electronic properties as well as on ε .

In fact, the large range of values for ε found by different experiments on graphene (Elias et al. 2011, Siegel et al. 2011, Bostwick et al. 2010, Reed et al. 2010, Wang et al. 2012, Sanchez-Yamagishi et al. 2012, Fallahazad et al. 2012, Jellison et al. 2007) and MoS₂ (Zhang et al. 2012, Kim et al. 2012, Bell et al. 1976, Frindt et al. 1963, Beal et al. 1979) has become a subject of considerable discussions. More factors, apart from the external electric fields and layer thickness, indicate that ε might depend on the underneath substrate as recently measured for graphene (Hwang et al. 2012) and MoS₂ layers (Bao et al. 2013). In practical terms, the dielectric constant is defined by $\varepsilon = (\varepsilon_{sub} + \varepsilon_{vac})/2$, with ε_{sub} and ε_{vac} the dielectric constant values for the substrate and vacuum, respectively. However, this approach suggests that the environment could play a role in the determination of the intrinsic dielectric constant of these 2D materials. Therefore, it is paramount to determine the intrinsic value of ε despite of external screening environments.

In the present Chapter, we provide a review of some of our recent computational studies on the effect of electric fields on multilayer graphene and MoS₂. We will consider both layered systems at different field magnitudes (0-1.0 V/Å) and number of layers (2L-10L). Some differences on the dielectric response between graphene and MoS₂ will be discussed based on simple electrostatic concepts, which will give generality to the calculations for other 2D-layers still to be explored.

2 Electrical Field Tuning of the Dielectric Constant

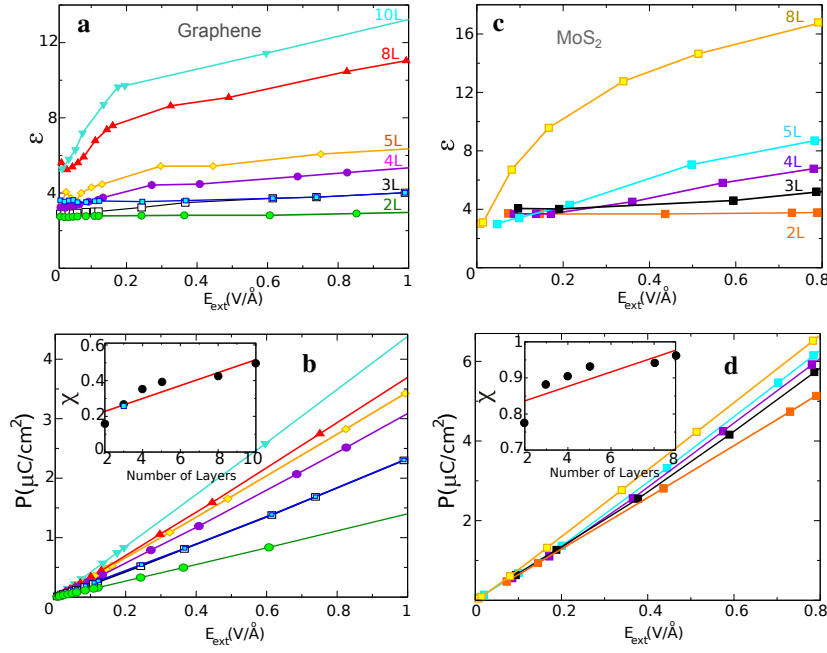


Fig. 1 Calculated ϵ and electric polarization $P(\mu\text{C}/\text{cm}^2)$ as a function of E_{ext} for graphene and MoS₂ structures. Results for graphene, **a** and **b**, and for MoS₂, **c** and **d**, are shown in the range of 2L–10L. The insets in **b**, and **d**, show the electric susceptibility χ versus the number of layers. A linear fitting is shown by the red line. Calculations for graphene were performed using the Bernal stacking order, which has not shown appreciable changes as compared to the Rhombohedral stacking. 3L is also shown in Rhombohedral stacking using filled blue squares in **a**. The Bernal stacking was used for all calculations on MoS₂. Adapted from (Santos et al. 2013a, Santos et al. 2013b).

Figure 1a, c display how ϵ evolves with external fields for different number of graphene and MoS₂ layers, respectively. At low fields, $E_{\text{ext}} \leq 0.001$

$\text{V}/\text{\AA}$, ε is almost independent of the number of layers having a value close to ~ 4 for both two-dimensional crystals. As the external field E_{ext} is increased, ε reaches larger values, up to $\varepsilon = 12.0$ at $E_{\text{ext}} = 1.0 \text{ V}/\text{\AA}$ for $N = 10$ graphene layers. Similar electric response is observed for MoS_2 with $\varepsilon = 16.8$ at $E_{\text{ext}} = 0.8 \text{ V}/\text{\AA}$ for $N = 8$ layers with an approximately linear dependence of ε on the number of layers at a fixed magnitude of the field. These values for ε are in good agreement with those found by experimental groups working on graphene (Elias et al. 2011, Siegel et al. 2011, Bostwick et al. 2010, Reed et al. 2010, Wang et al. 2012, Sanchez-Yamagishi et al. 2012, Fallahazad et al. 2012, Jellison et al. 2007) and on MoS_2 (Zhang et al. 2012, Kim et al. 2012, Bell et al. 1976, Frindt et al. 1963, Beal et al. 1979) samples. The electric susceptibility χ extracted from the polarization P clearly shows the roughly linear dependence on the number of layers N as plotted in Fig. 1b, d. Moreover, the comparison between graphene and MoS_2 also gives that the tuning of ε with the external field is larger to the latter. At $N = 8$, χ is $\chi = 0.95$ for multilayer MoS_2 and $\chi = 0.42$ for multilayer graphene, which is less than half of that value calculated for MoS_2 . This suggests that the dichalcogenide layer is more electrically polarizable than graphene.

We note that electric fields of the magnitude considered here can in principle be experimentally created, as recently obtained in the case of 3L graphene (Zou et al. 2013) which fields close to $\sim 0.6 \text{ V}/\text{\AA}$ were achieved taking into account HfO_2 gates. In the case of MoS_2 , the high dielectric breakdown, due to the chemical character of the Mo–S covalent bonds, allows the application of large electric bias as recently reported in voltage-current measurements (Lembke et al. 2012).

3 Interlayer Electric Field: Spatial Dependence

Next we discuss the origin of the electric-field mediated tunable dielectric constant in graphene and MoS_2 layered systems. Figure 2 shows the electric response in terms of the effective electric field E_{eff} calculated from the Hartree potential V_H along the supercell for bilayer structures. The application of the external field E_{ext} generates an interlayer charge-transfer which partially cancels E_{ext} inducing the appearance of E_{eff} in the region between the layers. At low E_{ext} , all the induced values of E_{eff} are approximately constant, within the numerical accuracy of our model, assuming similar shapes as displayed in the dark regions of Fig. 2a,c. At fields close to those used to modify the band gap of 2L graphene (Mak et al. 2009, Zhang et al. 2009, Castro et al. 2007), or used in MoS_2 transistors (Radisavljevic et al. 2011), that is $E_{\text{ext}} = 0.08 \text{ V}/\text{\AA}$, the effective field E_{eff} is already dependent on position z , with a maximum at the mid-point between the layers. MoS_2 has the difference to be formed by S–Mo–S bonds perpendicular to the external field, which induce a smaller but finite contribution between the S atoms. Moreover, the

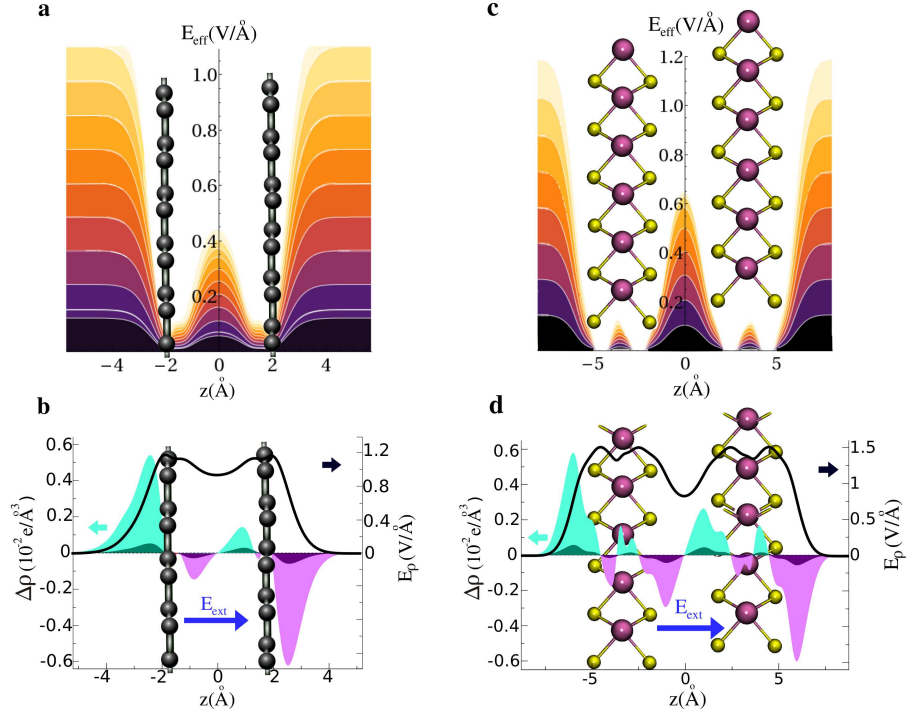


Fig. 2 Effective electric field E_{eff} calculated as a function of the interlayer distance at different external fields E_{ext} for **a**, bilayer graphene, and **c**, bilayer MoS₂. The color gradient shows the evolution from low (dark color) to high (bright color) values of the applied electric fields. Induced charge densities, $\Delta\rho = \rho(E_{\text{ext}}) - \rho(0)$, in $e/\text{Å}^3$, between the **b**, carbon surfaces and the **d**, MoS₂-planes. For graphene, the bolder and lighter shaded curves correspond to $E_{\text{ext}} = 0.12 \text{ V/Å}$ and $E_{\text{ext}} = 1.22 \text{ V/Å}$, respectively. The solid black curve corresponds to the electric field generated by the induced charge, E_p , at $E_{\text{ext}} = 1.22 \text{ V/Å}$. For MoS₂, the bolder and lighter shaded curves correspond to $E_{\text{ext}} = 0.14 \text{ V/Å}$ and $E_{\text{ext}} = 1.5 \text{ V/Å}$, respectively. The solid black curve corresponds to E_p at $E_{\text{ext}} = 1.5 \text{ V/Å}$. The large blue arrow shows the direction of E_{ext} relative to the bilayer structures. Adapted from (Santos et al. 2013a, Santos et al. 2013b).

effective field on 2L MoS₂ assumes a narrower shape relative to graphene with negligible values close to S. The electric response can also be analyzed based on the induced charge densities, $\Delta\rho$, at different fields as plotted in Figure 2b,d. Both layered systems show a charge accumulation at the layer that is under positive potential $+V$ and a corresponding depletion at the other one $-V$. The integration of $\Delta\rho$ along z , utilizing the Poisson equation $\nabla^2 V(z) = -\Delta\rho/\epsilon_0$, where ϵ_0 is the vacuum permittivity, results in a response electric field E_p (solid black line in Figure 2b,d) that screens the external electric field, that is, $E_{\text{eff}} \approx E_{\text{ext}} - E_p$.

4 Electric Field Damping in Multilayer Systems

In the previous section, we have considered in detail the electric response due to external fields on graphene and MoS₂ 2L structures. Although this is an important system, other aspects are also crucial to understand and control the screening associated to two-dimensional crystals. For example, one needs to explore the characteristics of multilayer systems subjected to external bias, as well as the possibility to compare structures with different electronic character. This kind of knowledge is instrumental in possible applications in electronics and optoelectronics.

We address next the dependence of ε as a function of the number of graphene and MoS₂ layers N as shown in Figure 3. Despite the electronic character of each system, the application of E_{ext} on thicker structures creates higher E_{eff} in the first few layers with a reduction of field in the innermost regions of the structure. For example in graphene, in the $N = 10$ case, the maximum value of E_{eff} between the two carbon layers at $z = 3z_o$ and $4z_o$ is 3.2 times larger than that between the layers at $z = 2z_o$ and $3z_o$. In deeper layers, the field decays further reaching even smaller values. For MoS₂, the outermost layers show a slightly higher E_{eff} and the field decay follows that observed for graphene. However, the damping between internal and external layers, that is, those closer to the gate bias, is slightly different as that observed at the carbon planes. This suggests that the charge polarization of the layers due to the different electronic character (Fig. 1c,d) plays an important role on the screening behavior and also on the electrical tuning of the dielectric constant with the number of layers. As ε is calculated by the ratio of the external and internal fields to the slabs, the enhancement in the value of the dielectric constant with the number of layers N is directly related to the reduction of the field in the innermost regions of the structure which leads to lower ε values for lower values of N . This decay of field with the layer thickness is in good agreement with recent electrostatic force microscopy and Kelvin probe microscope measurements performed for MoS₂ (Castellanos-Gomez et al. 2013, Li et al. 2013) and graphene (Datta et al. 2009).

5 Electrostatic Exfoliation on Graphene and MoS₂ Layers

In this section we analyze the possibility to use an electrostatic gate that can be used to exfoliate graphene and MoS₂ layers at different bias. We note that there is an upper limit on the magnitude of E_{ext} that can be applied to the systems as the bias induces a shift of the equilibrium position of the layers to higher interlayer separations. Figure 4 displays the total

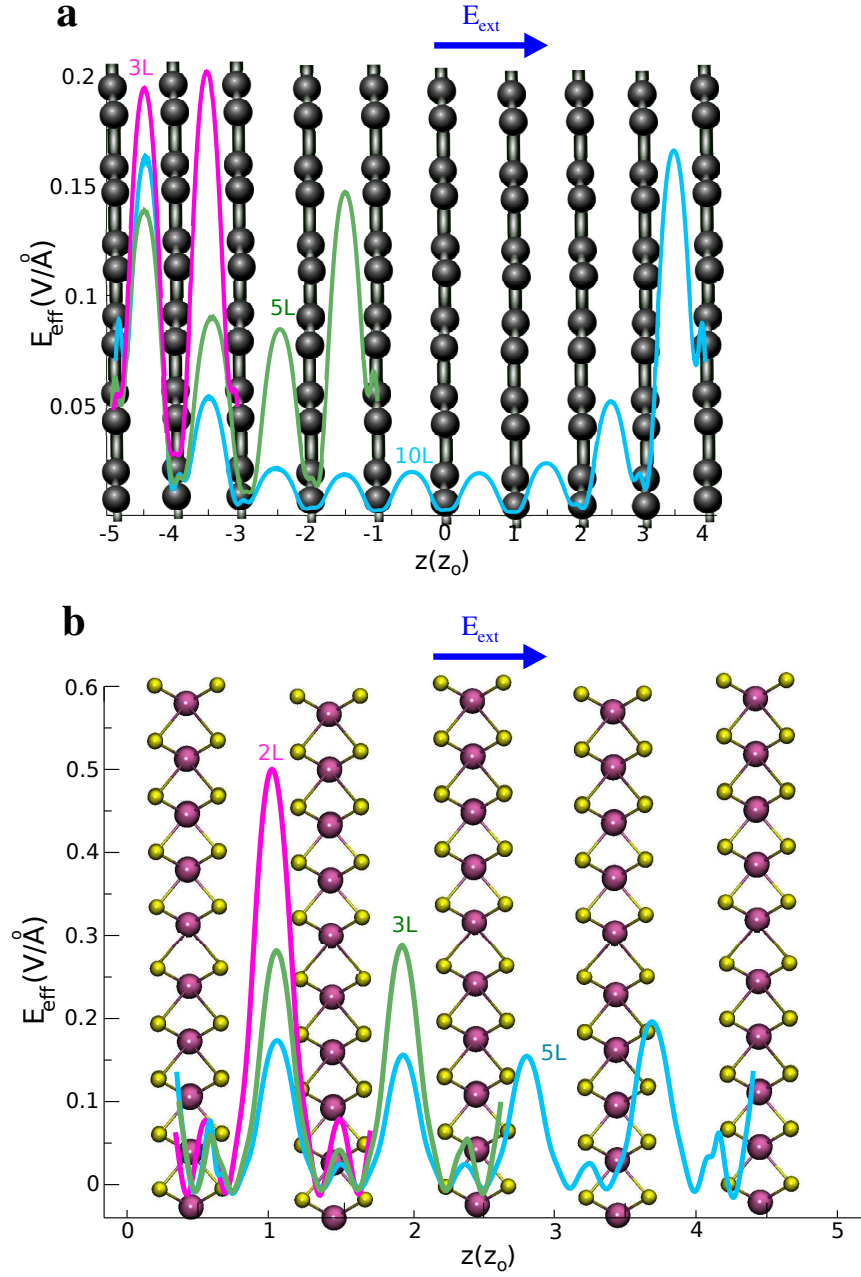


Fig. 3 Effective electric field E_{eff} as a function of the interlayer position z_o for **a**, 3L-10L graphene and **b**, 2L-5L MoS₂. Note that z_o assumes different values for graphene ($z_o = 3.41 \text{ \AA}$) and MoS₂ ($z_o = 6.70 \text{ \AA}$). Geometries are shown on the background on each panel. The applied fields are $0.50 \text{ V}/\text{\AA}$ and $0.73 \text{ V}/\text{\AA}$ for graphene and MoS₂, respectively. The blue arrow indicates the relative orientation of E_{ext} . Adapted from (Santos et al. 2013a, Santos et al. 2013b).

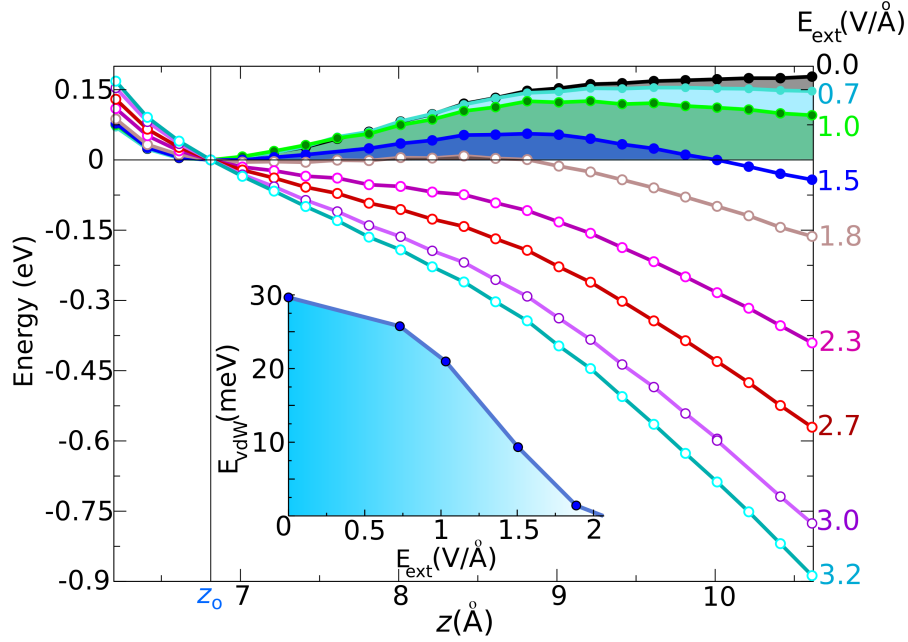


Fig. 4 Energy per MoS₂ unit cell as a function of interlayer distance for different values of E_{ext} (V/Å). The vertical solid line indicates the equilibrium interlayer distance $z_0 = 6.70$ Å. The inset shows the van der Waals barrier (E_{vdW}) per atom as a function of E_{ext} . Adapted from (Santos et al. 2013b).

energy for MoS₂ 2L as a function of the interlayer distance z . We focus on MoS₂ since similar effects are observed for graphene. At $E_{\text{ext}} = 0.0$ V/Å, a van der Waals barrier E_{vdW} of 30 meV/atom prevents the separation of the two layers from z_0 to infinity. At finite E_{ext} , the value of E_{vdW} decreases, indicating that the MoS₂-layers become less bound. At $E_{\text{ext}} = 2.0$ V/Å, the two dichalcogenide layers can be easily separated with a barrier of only 0.45 meV/atom. This indicates that an electrostatic gate can be utilized for exfoliating and printing few-layers MoS₂ in pre-pattern form similarly to that observed for graphene (Lian et al. 2009). Since several challenges of making industrially available large-scale areas of 2D-crystals and fabricating atomic features with precise electronic structure are still to be overcome, the electrostatic exfoliation shown in our calculations could open new avenues for the achievement of such desired properties.

6 Conclusions

In this Chapter we have reviewed the electrical response of two representative layered materials for future devices-based on graphene and MoS₂. We have focused on the interplay between electric fields and screening properties of few-layer structures. Density functional theory was the main tool used to compute the properties of the analyzed systems. We have used simple models to understand the observed trends. In particular, we find that the effective dielectric constant of graphene and MoS₂ is electrically tunable, with the layer thickness playing an important role in the enhancement of the effect. The thicker the structure is, the stronger the modulation with electric fields. The driving force for such behavior is due to the linear dependence of the electrical polarization of the layers on the external field. The response field computed from the polarization charge does not screen completely the external bias, which generate higher interlayer fields at thinner structures. Differences due to semi-metallic and semiconducting electronic character of the layers are observed in terms of the field damping inside of the compounds: graphene tends to screen the external field at the outermost layers of system, while MoS₂ the field penetrates deeper in the layers. These results are in sound agreement with recent experiments performed for both materials.

We have also explored the possibility to control the layer exfoliation using electric fields. We have found that the induced interlayer charge imbalance generated by the bias can drive the system to an unstable state where the layers can be separated from each other. The interlayer equilibrium position is modified as a function of the field magnitude, which induces a reduction of the van der Waals barrier that keeps the layers together. As a result, there are variations of the interlayer separations even at low-fields. This investigation is highly relevant in the interpretation of experimental results underway since the field of 2D-materials is just in its beginning where several techniques and effects are still to be developed and explored.

References

1. Castro Neto, A. H., Guinea, F., Peres, N. M. R., Novoselov, K. S., Geim, A. K. The electronic properties of graphene. *Rev. Mod. Phys.* **2009**, *81*, 109-162.
2. Wang, Q. H.; Kalantar-Zadeh, K.; Kis, A.; Coleman, J. N.; Strano, M. S. Electronics and Optoelectronics of Two-dimensional Transition Metal Dichalcogenides. *Nat. Nanotechnol.* **2012**, *7*, 699-712.
3. Castro, E. V., Novoselov, K. S., Morozov, S. V., Peres, N. M. R., dos Santos, J. M. B. Lopes, Nilsson, J., Guinea, F., Geim, A. K., Castro-Neto, A. H. Biased Bilayer Graphene: Semiconductor with a Gap Tunable by the Electric Field Effect. *Phys. Rev. Lett.* **2007**, *99*, 216802-216806.
4. Mak, K. F.; Lee, C.; Hone, J.; Shan, J.; Heinz, T. F. Atomically Thin MoS₂: a New Direct-Gap Semiconductor. *Phys. Rev. Lett.* **2010**, *105*, 136805-136809.

5. Elias, D. C., Gorbachev, R. V., Mayorov, A. S., Morozov, S. V., Zhukov, A. A., Blake, P., Ponomarenko, L. A., Grigorieva, I. V., Novoselov, K. S., Guinea, F., Geim, A. K. Dirac cones reshaped by interaction effects in suspended graphene. *Nature Phys.* **2011**, *7*, 701-704.
6. Siegel, D. A., Park, C. H., Hwang, C. Deslippe, J., Fedorov, A. V., Louie, S. G., Lanzara, A. Many-body interactions in quasi-freestanding graphene. *Proceedings of the National Academy of Sciences* **2011**, *108*, 11365-11370.
7. Bostwick, A., Speck, F., Seyller, T., Horn, K., Polini, M., Asgari, R., MacDonald, Allan H., Rotenberg, E. Observation of Plasmarons in Quasi-Freestanding Doped Graphene. *Science* **2010**, *328*, 999-1002.
8. Reed, J. P., Uchoa, B., Joe, Y. I., Gan, Y., Casa, D., Fradkin, E., Abbamonte, P. The Effective Fine-Structure Constant of Freestanding Graphene Measured in Graphite. *Science* **2010**, *330*, 805-808.
9. Wang, Y., Brar, V. W., Shytov, A. V., Wu, Q., Regan, W., Tsai, H. Z., Zettl, A., Levitov, L. S., Crommie, M. F. Mapping Dirac Quasiparticles near a Single Coulomb Impurity on Graphene. *Nature Phys.* **2012**, *8*, 653-657.
10. Sanchez-Yamagishi, J. D., Taychatanapat, T., Watanabe, K., Taniguchi, T., Yacoby, A., Jarillo-Herrero, P. Quantum Hall Effect, Screening, and Layer-Polarized Insulating States in Twisted Bilayer Graphene. *Phys. Rev. Lett.* **2012**, *108*, 076601-076606.
11. Fallahazad, B., Hao, Y., Lee, K., Kim, S., Ruoff, R. S., Tutuc, E. Quantum Hall effect in Bernal stacked and twisted bilayer graphene grown on Cu by chemical vapor deposition. *Phys. Rev. B* **2012**, *85*, 201408-201413.
12. Jellison, G. E., Hunn, J. D., Lee, Ho N. Measurement of optical functions of highly oriented pyrolytic graphite in the visible. *Phys. Rev. B* **2007**, *76*, 085125-085133.
13. Zhang, X.; Hayward, D. O.; Mingos, D. M. P. Dielectric Properties of MoS₂ and Pt Catalysts: Effects of Temperature and Microwave Frequency. *Catal. Lett.* **2002**, *84*, 225-233.
14. Kim, S.; Konar, A.; Hwang, W. S.; Lee, J. H.; Lee, J.; Yang, J.; Jung, C.; Kim, H.; Yoo, J. B.; Choi, J. Y.; *et al.* High-Mobility and Low-Power Thin-Film Transistors Based on Multilayer MoS₂ Crystals. *Nat. Commun.* **2012**, *3*, 1011-1018.
15. Bell, M. G.; Liang, W. Y. Electron Energy Loss Studies in Solids: The Transition Metal Dichalcogenides. *Adv. Phys.* **1976**, *1976*, 53-86.
16. Frindt, R. F.; Yoffe, A. D. Physical Properties of Layer Structures: Optical Properties and Photoconductivity of Thin Crystals of Molybdenum Disulphide. *Proc. Roy. Soc. A* **1963**, *273*, 69-83.
17. Beal, A. R.; Hughes, H. P. Kramers-Kronig Analysis of the Reflectivity Spectra of 2H-MoS₂, 2H-MoSe₂ and 2H-MoTe₂. *J. Phys. C: Solid State Phys.* **1979**, *12*, 881-890.
18. Hwang, C., - Siegel, David A., Mo, S. K., Regan, W., Ismach, A., Zhang, Y., Zettl, A., Lanzara, A. Fermi velocity engineering in graphene by substrate modification. *Sci. Rep.* **2012**, *2*:590.
19. Bao, W.; Cai, X.; Kim, D.; Sridhara, K.; Fuhrer, M. S. High Mobility Ambipolar MoS₂ Field-Effect Transistors: Substrate and Dielectric Effects. *Appl. Phys. Lett.* **2013**, *102*, 042104-042108.
20. Santos, E. J. G.; Kaxiras, E. Electric-Field Dependence of the Effective Dielectric Constant in Graphene. *Nano Lett.* **2013**, *13*, 898-902.
21. Santos, E. J. G.; Kaxiras, E. Electrically-Driven Tuning of the Dielectric Constant in MoS₂ Layers. *ACS Nano* **2013**, *7*, 10741-10746.
22. Zou, K.; Zhang, Fan; Clapp, C.; MacDonald, A. H.; Zhu, J. Transport Studies of Dual-Gated ABC and ABA Trilayer Graphene: Band Gap Opening and Band Structure Tuning in Very Large Perpendicular Electric Fields. *Nano Lett.* **2013**, *13*, 369-373.
23. Lembke, D.; Kis, A. Breakdown of High-Performance Monolayer MoS₂ Transistors. *Nano Lett.* **2012**, *6* 10070-10075.
24. Radisavljevic, B.; Radenovic, A.; Brivio, J.; Giacometti, V.; Kis, A. Single-Layer MoS₂ Transistors. *Nat. Nanotechnol.* **2011**, *6*, 147-150.

25. Mak, K. F., Lui, C. H., Shan, J., Heinz, T. F. Observation of an Electric-Field-Induced Band Gap in Bilayer Graphene by Infrared Spectroscopy. *Phys. Rev. Lett.* **2009**, *102*, 256405-256409.
26. Zhang, Y., Tang, T. T., Girit, C., Hao, Z., Martin, M. C., Zettl, A., Crommie, M. F., Shen, Y. R., Wang, F. Direct observation of a widely tunable bandgap in bilayer graphene. *Nature* **2009**, *459*, 820-823.
27. Castellanos-Gomez, A.; Cappelluti, E.; Roldán, R.; Agrait, N.; Guinea, F.; Rubio-Bollinger, G. Electric-Field Screening in Atomically Thin Layers of MoS₂: the Role of Interlayer Coupling. *Adv. Mater.* **2013**, *25*, 899-903.
28. Li, Y.; Xu, C.-Y.; Zhen, L. Surface Potential and Interlayer Screening Effects of Few-Layer MoS₂ Nanoflakes. *Appl. Phys. Lett.* **2013**, *102*, 143110-143114.
29. Datta, S. S.; Strachan, D. R.; Mele, E. J.; Johnson, A. T. C. Surface Potentials and Layer Charge Distributions in Few-Layer Graphene Films. *Nano Lett.* **2009**, *9*, 7-11.
30. Liang, X., Chang, A. S. P., Zhang, Y., Harteneck, B. D., Choo, H., Olynick, D. L., Cabrini, S. Electrostatic Force Assisted Exfoliation of Prepatterned Few-Layer Graphenes into Device Sites. *Nano Letters* **2009**, *9* 467-472.